Environmental Research Letters

LETTER

# Impacts of ocean albedo alteration on Arctic sea ice restoration and Northern Hemisphere climate

**Ivana Cvijanovic**[1,3], **Ken Caldeira**[1] **and Douglas G MacMartin**[2]

[1] Carnegie Institution for Science, Department of Global Ecology, 260 Panama St., Stanford, CA 94305, USA
[2] California Institute of Technology, Department of Computing + Mathematical Sciences, 1200 E. California Blvd., Pasadena, CA 91125, USA
[3] Atmospheric, Earth and Energy Division, Lawrence Livermore National Laboratory, 7000 East Avenue, Livermore, CA 94550, USA

**E-mail:** ivanacv@llnl.gov

**Keywords:** Arctic sea ice restoration, ocean albedo alteration, atmospheric impacts

Supplementary material for this article is available online

**OPEN ACCESS**

**RECEIVED**
25 January 2015

**REVISED**
20 February 2015

**ACCEPTED FOR PUBLICATION**
26 March 2015

**PUBLISHED**
28 April 2015



## Abstract

The Arctic Ocean is expected to transition into a seasonally ice-free state by mid-century, enhancing Arctic warming and leading to substantial ecological and socio-economic challenges across the Arctic region. It has been proposed that artificially increasing high latitude ocean albedo could restore sea ice, but the climate impacts of such a strategy have not been previously explored. Motivated by this, we investigate the impacts of idealized high latitude ocean albedo changes on Arctic sea ice restoration and climate. In our simulated 4x$CO_2$ climate, imposing surface albedo alterations over the Arctic Ocean leads to partial sea ice recovery and a modest reduction in Arctic warming. With the most extreme ocean albedo changes, imposed over the area 70°–90°N, September sea ice cover stabilizes at ~40% of its preindustrial value (compared to ~3% without imposed albedo modifications). This is accompanied by an annual mean Arctic surface temperature decrease of ~2 °C but no substantial global mean temperature decrease. Imposed albedo changes and sea ice recovery alter climate outside the Arctic region too, affecting precipitation distribution over parts of the continental United States and Northeastern Pacific. For example, following sea ice recovery, wetter and milder winter conditions are present in the Southwest United States while the East Coast experiences cooling. We conclude that although ocean albedo alteration could lead to some sea ice recovery, it does not appear to be an effective way of offsetting the overall effects of $CO_2$ induced global warming.

## 1. Introduction

Arctic sea ice loss plays a central role in the amplification of Arctic warming (Screen and Simmonds 2010) and can affect atmospheric circulation patterns across the Northern Hemisphere (Chapman and Walsh 2007, Budikova 2009, Francis *et al* 2009, Screen *et al* 2013, Vihma 2014). Arctic marine ecosystems and human settlements adjacent to the Arctic seas are highly dependent on sea ice cover, with sea ice decline leading to habitat range changes, biodiversity loss, shifts in traditional lifestyles and relocation of indigenous communities (Larsen *et al* 2014). Climate projections of Arctic temperatures and sea ice extent (Wang and Overland 2012, Kirtman *et al* 2013) indicate that ecological and socio-economical pressures in the Arctic region are likely to become more severe in the coming decades. Additional concerns related to enhanced Arctic warming include global sea level rise (Church *et al* 2013) and the exacerbation of greenhouse gas forcing due to permafrost thaw and methane release (Knorr *et al* 2005).

It has been suggested that some of the consequences of global warming (e.g., sea ice loss) could be partially offset by the application of technological approaches (Shepherd 2009). The most commonly investigated methods are stratospheric aerosol injections, aimed at offsetting the global effects of $CO_2$ radiative forcing by decreasing absorption of sunlight, i.e., by decreasing net incoming solar radiation at the *top* of atmosphere (Crutzen 2006, Caldeira and Wood 2008, Robock *et al* 2008, Tilmes *et al* 2014). Brightening marine clouds has also been investigated as an approach to increase planetary albedo (Latham

*et al* 2012). *Surface* albedo modification methods have been considerably less explored, and when they have, solely in terms of impacts of land albedo modifications on global warming (Ridgwell *et al* 2009, Singarayer *et al* 2009, Irvine *et al* 2011). In recent years, several methods aimed at ocean albedo alteration have been proposed. For example Seitz (2011) suggested hydrosol (microbubble) injection and stabilization as a means of increasing the reflectivity of the ocean surface that would in turn, increase the planetary albedo and offset the effects of $CO_2$ radiative forcing. Field *et al* (2012), focused on sea ice restoration and investigated implementation of floating granular materials with low subsidiary environmental impact that would reduce the solar heat absorption in the underlying water and aid sea ice recovery.

The technological feasibility and large scale application of methods aimed at ocean albedo alteration remains highly uncertain. Interestingly, the climate impacts of these conceptually new strategies are not well understood either, lacking a comprehensive climate model analysis that explores the physical limitations of high latitude ocean albedo alteration. Motivated by this, in the current study we focus on understanding the physical (climate) impacts of ocean surface albedo alteration in the Arctic. We investigate the climate response to an idealized scenarios in which albedo over a large area in the Arctic Ocean has been substantially increased. Such extreme scenarios are not intended to simulate a specific real world application, but to understand the climate response at the upper limit of albedo forcing.

We investigate the effects of altered ocean albedo on Arctic sea ice recovery and Northern Hemisphere climate using the Community Earth System Model (CESM) (Gent *et al* 2011). Ocean albedo changes are introduced in a seasonally ice free $4xCO_2$ climate, with ~10 °C warmer Arctic (annual mean) relative to the pre-industrial conditions (supplementary table 1 available at stacks.iop.org/ERL/10/044020/mmedia). For reference, a $4xCO_2$ concentration (1138.8 ppm) is less than the end of the century $CO_2$ equivalent concentration in the RCP8.5 scenario (1370 ppm) (Vuuren *et al* 2011). In simulations with altered albedo, ocean albedo is set uniformly to 0.9 over the following regions: 65°–90°N, 70°–90°N, 75°–90°N, 80°–90°N and 70°–80°N (see section 2 for details). In comparison, the albedo of snow covered sea ice surface ranges between 0.8 and 0.9 (Allison *et al* 1993, Perovich *et al* 2002, 1998). In order to briefly illustrate the dependence of the sea ice response and global mean temperatures on the strength of the imposed albedo changes we also discuss three additional scenarios in which ocean albedo over the area 70°–90°N is set uniformly to 0.7 and 0.8.

In the proceeding analysis, we first investigate if extreme scenarios of ocean albedo alteration can lead to sea ice recovery and decreased global warming (under increased atmospheric $CO_2$ concentrations). This is followed by a discussion of local and remote climate responses and consideration of high latitude energy budget changes.

## 2. Methods

The simulations have been performed using the National Center for Atmospheric Research' Community Earth System Model (CESM) (Gent *et al* 2011) version 1.0.4. In our configuration, the model incorporates the Community Atmosphere Model version 4 (Neale *et al* 2013), Community Land Model version 4 (Lawrence *et al* 2011), Los Alamos Sea Ice Model version 4 (Community Ice CodeE 4—CICE4) (Hunke and Lipscomb 2008) and Parallel Ocean Program version 2 (Smith *et al* 2010, Danabasoglu *et al* 2011). The atmosphere and land model are run using a 1.9° × 2.5° (latitude × longitude) finite volume grid with 26 atmospheric levels in the vertical dimension. The ice and ocean models are defined on a 1° displaced pole grid (gx1v6). Our model configuration reproduces well the observed mean and seasonal cycle of the Arctic sea ice extent as described by Gent *et al* (2011) and Wang and Overland (2012) (tested in the framework of the Community Climate System Model version 4). Relative to the earlier model version (namely the Community Climate System Model version 3, Collins *et al* 2006), the model used in this study was shown to feature substantial improvements in representation of ocean meridional overturning circulation and sea surface temperatures over the major upwelling regions as well as major improvements in representation of Arctic sea ice concentrations and albedo values (Danabasoglu and Gent 2009, Danabasoglu *et al* 2011, Gent *et al* 2011). However, biases remain with regards to the excessive low cloud cover in the Arctic and the latitudinal distribution of cloud forcing (Gent *et al* 2011).

In the control ('$1xCO_2$') simulation, solar insolation, orbital parameters and greenhouse gas forcing are set to their pre-industrial values ($CH_4$ = 791.6 ppb, $CO_2$ = 284.7 ppm, $N_2O$ = 275.68 ppb). In the $4xCO_2$ simulation, all parameters, except for the $CO_2$ forcing of 1138.8 ppm which is applied instantaneously, are unchanged from the control simulation. Ocean and ice restart files used to initialize the $4xCO_2$ simulation are obtained from year 200 of an abrupt $4xCO_2$ CESM simulation (Gent *et al* 2011). The $1xCO_2$ and $4xCO_2$ simulations were run for 150 years. The last 30 years of these simulations were used in the analysis.

Altered ocean albedo simulations are branched from year 100 of the fully coupled $4xCO_2$ simulation and run for 50 years. In the altered ocean albedo simulations, both direct and diffuse components of ocean albedo have been uniformly modified over the selected regions and set equal to 0.9. We ran five main simulations, in which we alter the ocean albedo within the following regions: 65°–90°N, 70°–90°N, 75°–90°N, 80°–90°N and 70°–80°N; we refer to these simulations

**Table 1.** Experiment summary.

| Simulation name | $CO_2$ concentration (ppm) | Altered ocean albedo region (degrees latitude) | Prescribed ocean albedo value (−) |
|---|---|---|---|
| 1x$CO_2$ | 284.7 | — | — |
| 4x$CO_2$ | 1138.8 | — | — |
| alb65–90N | 1138.8 | 65.4°–90°N | 0.9 |
| alb70–90N | 1138.8 | 71.1°–90°N | 0.9 |
| alb75–90N | 1138.8 | 76.7°–90°N | 0.9 |
| alb80–90N | 1138.8 | 80.5°–90°N | 0.9 |
| alb70–80N | 1138.8 | 71.1°–78.6°N | 0.9 |
| alb70–90Nval08 | 1138.8 | 71.1°–90°N | 0.8 |
| alb70–90Nval07 | 1138.8 | 71.1°–90°N | 0.7 |

as alb65–90N, alb70–90N, alb75–90N, alb80–90N and alb70–80N, respectively. In addition, we perform three additional simulations with albedo changes imposed over the area 70°–90°N and ocean albedo set to equal 0.7 and 0.8. These simulations are referred to as alb70–90Nval07 and alb70–90Nval08, respectively. The simulations are summarized in table 1. The strength or spatial coverage of albedo alterations tested are not chosen having in mind any practical implementation. We choose these extreme scenarios to qualitatively study physical implications close to the limit of albedo changes. Unless noted differently, all values are shown as a mean ± one standard error calculated over the last 30 years of model simulation. In cases where the uncertainty ranges are not shown, the estimated uncertainty is $<0.5 \times 10^{-N}$, where $N$ is the number of digits to the right of the decimal point.

We use the last 30 years in our analysis, as this is sufficient to minimize effects from the variability while avoiding the initial transient. Over the time period considered, the atmosphere is in equilibrium with the achieved ocean state. Our simulations are, however, not long enough to account for ocean adjustment much beyond the upper mixed layer. Deep-ocean adjustments following $CO_2$ quadrupling require several thousand years to reach equilibrium (Li *et al* 2013). Thus, the model response and sensitivity to ocean albedo alteration may differ over longer (i.e., millennial) time-scales.

Atmospheric heat transport (AHT) and its components are calculated following the previously documented heat transport calculations with the CESM model (Kay *et al* 2012), assuming no storage of heat in the atmosphere on the timescale of the experiments. Fluxes are reported as area-weighted sums (PW) to allow direct comparison between energy budget changes (surface and top-of-atmosphere (TOA)) and AHT changes over/into the selected region. We use 'TOA' to refer to fluxes at the top of the model atmosphere. When referring to the area 60°–90°N we actually consider the area 61.6°N–90°N.

## 3. Results

Imposing ocean albedo alterations in our model simulations resulted in increased sea ice area and decreased Arctic warming (figures 1(a) and (b), supplementary figure 1(a) available at stacks.iop.org/ERL/10/044020/mmedia). Sea ice recovery occurs largely in the first two decades after imposing the albedo alterations with no detectable trend in sea ice area after the first two decades of deployment. The largest sea ice recovery is accomplished in the seasons experiencing the largest Arctic sea ice decline in the absence of ocean albedo changes: autumn and winter (supplementary figure 1(b) available at stacks.iop.org/ERL/10/044020/mmedia). In the simulation with albedo alterations imposed over 70°–90°N (alb70–90N), September sea ice area equals $3.17 \pm 0.16$ million km$^2$ (~40% of preindustrial 1x$CO_2$ extent) compared to $0.28 \pm 0.04$ million km$^2$

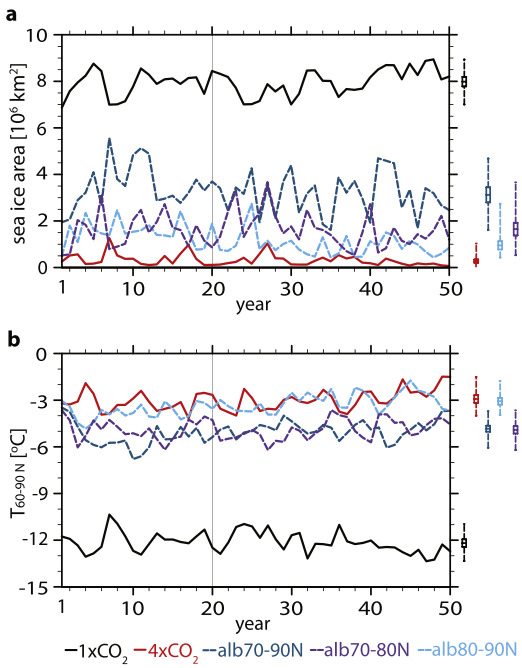


**Figure 1.** (a) September Arctic sea ice areas and (b) annual mean surface air temperatures averaged over the area (60°–90°N) over the last 50 years of model integration. 1x$CO_2$ simulation—black solid line, 4x$CO_2$ simulation—red solid line, alb70–90N—dark blue dashed line, alb80–90N—light blue dashed line, alb70–80N—dark purple dashed line. Boxes on the right show the mean with two standard errors while whiskers indicate min/max range (over the last 30 years). Both the sea ice area and surface air temperature stabilize within the first 20 years.

(~3% of preindustrial extent) in the 4xCO$_2$ simulation with no albedo modifications (figure 1(a)). Annual mean sea ice area in alb70–90N equals 74% of its preindustrial value, compared to 51% in the 4xCO$_2$ simulation with no albedo modifications. Variability in September and annual sea ice area increases in simulations with imposed albedo alterations relative to the 4xCO2 simulation (figure 1(a) and supplementary figure 1(a) available at stacks.iop.org/ERL/10/044020/mmedia). Annual mean and September sea ice area changes are summarized in supplementary table 1 available at stacks.iop.org/ERL/10/044020/mmedia.

Over the area 60°–90°N, annual average surface albedo (including land areas) increases from 0.38 ± 0.02 in the 4xCO$_2$ simulation to 0.49 ± 0.01 in alb70–90N, in comparison to 0.52 ± 0.02 in the 1xCO$_2$ simulation. High latitude albedo changes in other altered albedo simulations are summarized in supplementary table 2 available at stacks.iop.org/ERL/10/044020/mmedia. Despite the increased sea ice variability, the year to year high latitude surface albedo variability is decreased. This occurs because of the diminished contrast between ocean and sea ice albedo in the albedo modified case. At the model's TOA, over the area 60°–90°N imposed ocean albedo changes in alb70–90N result in TOA albedo of 0.53 ± 0.01 (compared to 0.54 ± 0.01 and 0.50 ± 0.01 in 1xCO$_2$ and in 4xCO$_2$ simulations respectively). The high latitude TOA albedo increase in alb70–90N relative to 4xCO$_2$ is thus only about 25% of the corresponding surface albedo increase, indicating a strong attenuation of surface albedo changes by the atmosphere, in agreement with previous studies (Donohoe and Battisti 2011). In comparison, clear-sky TOA albedo increase is ~65% of clear-sky surface albedo increase. High latitude albedo values are given in supplementary table 2 available at stacks.iop.org/ERL/10/044020/mmedia. Surface and TOA high latitude flux changes due to imposed ocean albedo alterations are discussed in the supplementary material, sections a–c available at stacks.iop.org/ERL/10/044020/mmedia.

Globally, imposed surface ocean albedo changes made no substantial impact on planetary albedo values (supplementary table 3 available at stacks.iop.org/ERL/10/044020/mmedia). Southern hemispheric TOA albedo values did not adjust to minimize hemispheric albedo asymmetries due to Northern hemispheric albedo changes, lending no support to the conjecture that cloud adjustments cause the two hemispheres to approach the same albedo regardless of the hemispheric difference in surface albedos (Voigt *et al* 2014).

One measure of the efficacy of imposed albedo alterations is the ratio of recovered annual mean sea ice area to the altered annual mean ocean albedo area (figure 2(a)). We find the ratios of recovered sea ice area to altered ocean albedo area to range from 46% (with modifications imposed over 80°–90°N) to 75% (70°–90°N) and 76% (75°–90°N). Ocean albedo

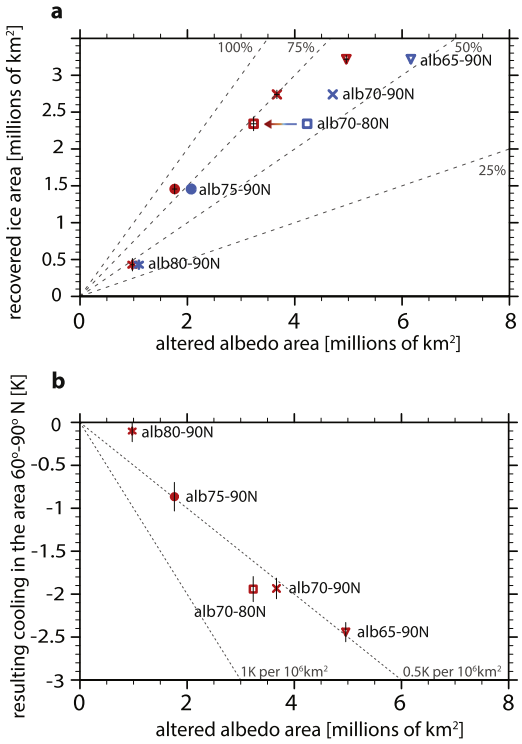


**Figure 2.** (a) Recovered annual mean ice area (km$^2$) versus altered annual mean ocean albedo area ($10^6$ km$^2$) relative to the control 4xCO$_2$ simulation calculated from the last 30 years of model integration (red points). Blue points indicate the initial altered ocean albedo area (mean value during the first year after imposing the albedo changes). Dashed lines show 25, 50, 75 and 100% efficacies (defined as ratio of recovered sea ice area per altered ocean albedo area). (b) Same as in (a) but for annual mean surface air temperature anomalies over 60°–90°N (K). Dashed lines indicate slopes of 1 K /$10^6$ km$^2$ and 0.5 K/$10^6$ km$^2$. The largest sea ice recovery per unit area of imposed ocean albedo changes is achieved in alb75–90N, while the largest high latitude cooling per unit area of imposed ocean albedo changes is accomplished in alb70–80N. (Data shown in panels (a) and (b) is also given in supplementary table 2.)

alteration over areas 75°–90°N, 70°–90°N and 70°–80°N recovers sea ice more efficiently than albedo alteration over 65°–90°N or 80°–90°N. In alb65–90N, the altered albedo area extends too far south for albedo changes to be effective in sea ice restoration (because of the higher temperatures). In contrast, in the case of alb80–90N, there is still much sea ice present (there is not much area of ocean left for albedo alterations to be imposed over) during the months when the albedo changes are able to achieve a substantial impact over the albedo altered latitudes. This demonstrates that the efficacy of sea ice restoration over certain areas depends on the achieved decrease in shortwave flux absorption and on the background temperatures (where it is sufficiently warm, no ice will form even with albedo modifications present). Imposed albedo modifications and sea ice recovery lead to relatively modest annual mean surface temperature decrease in the high latitudes: the largest annual mean cooling (achieved in alb65–90N) is ~2.5 K. High latitude (and global) annual mean cooling per unit altered

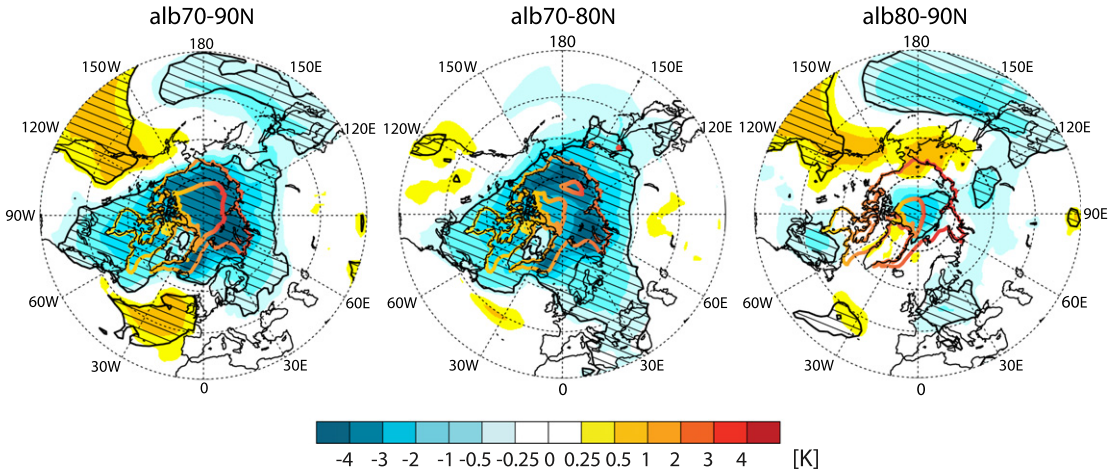


**Figure 3.** Annual surface air temperature anomalies (K) between 30° and 90°N in modified ocean albedo simulations relative to the control 4x$CO_2$ simulation. Dashed areas indicate the anomalies that are statistically significant at the 95% confidence level. In addition to the Arctic cooling, altered albedo simulations also show notable warming off the West Coast of North America (less pronounced in alb70–80N but still present). This pattern of temperature response is found in all simulations with imposed albedo modifications (see supplementary figure 3). Thin and thick contour lines indicate the areas with annual mean sea ice fractions larger than 15% and 80%, respectively.

albedo area is largest in the alb70–80N (figure 2(b) and supplementary figure 2 available at stacks.iop.org/ERL/10/044020/mmedia).

Although not as substantial as in the high latitudes, surface air temperature changes (following ocean albedo alteration) are also present over remote midlatitude regions indicating an influence of sea ice recovery on midlatitude circulation patterns. Midlatitude temperature changes are present in all simulations with modified ocean albedo (relative to the 4x$CO_2$ simulation) and consist of warming over the West Coast of North America and cooling over the East Coast of North America and parts of Europe (figure 3 and supplementary figures 3 and 4 available at stacks.iop.org/ERL/10/044020/mmedia).

This 'warm west—cold east' pattern over North America is strongest in the winter (supplementary figure 4 available at stacks.iop.org/ERL/10/044020/mmedia) and is accompanied by increased 500 hPa geopotential height over the western parts of North America and Siberia and decreased 500 hPa geopotential height over the North Pacific and eastern North America (relative to the 4x$CO_2$ simulation) (supplementary figure 5 available at stacks.iop.org/ERL/10/044020/mmedia). Similar spatial responses are found when considering sea level pressure anomalies (supplementary figure 6 available at stacks.iop.org/ERL/10/044020/mmedia), thus indicating an equivalent-barotropic response. This geopotential distribution allows for the propagation of cold polar air southward across the East Coast of the United States while maintaining mild winter conditions over the West Coast. Increased geopotential height over western North America stirs the wet tropical air southward, leading to wetter conditions in the midwest and drier conditions in the Northwest of the United States (supplementary figure 7 available at stacks.iop.org/ERL/10/044020/mmedia). Previous studies have suggested that Arctic sea ice loss can affect precipitation over western North America, resulting in drier conditions over the Southwest and wetter conditions over the Northwest of North America (Sewall 2005, Sewall and Sloan 2004). Our simulations support these findings by suggesting that the reverse change (Arctic sea ice recovery) will lead to drier conditions over the northern, and wetter conditions over the southern, parts of the United States's West Coast. However, this does not mean that sea ice recovery and sea ice loss result in reverse responses at all locations or in all fields. For example, over the northern parts of Asia, a number of studies have found positive geopotential height anomalies in response to the Arctic sea ice decline (e.g., Sewall 2005, Deser *et al* 2010, Peings and Magnusdottir 2014) as was the case in this study for sea ice recovery.

## 4. Discussion

A consideration of the energy budget changes over and into the area 60°–90°N (figure 4) allows for a better understanding of the causes of the remote responses in simulations with altered albedo modifications. Relative to the 4x$CO_2$ case, imposed albedo alterations lead to increased high latitude energy loss both at the surface and at the model's TOA.

High latitude surface net energy loss to the atmosphere in alb70–90N of $0.47 \pm 0.01$ PW, is equal to the 1x$CO_2$ value of $0.48 \pm 0.01$ PW (compared to $0.40 \pm 0.01$ PW in the 4x$CO_2$ simulation, supplementary table 4 available at stacks.iop.org/ERL/10/044020/mmedia). Increased surface net energy flux into the atmosphere in alb70–90N relative to 4x$CO_2$ is a result of a large increase in net shortwave flux from the

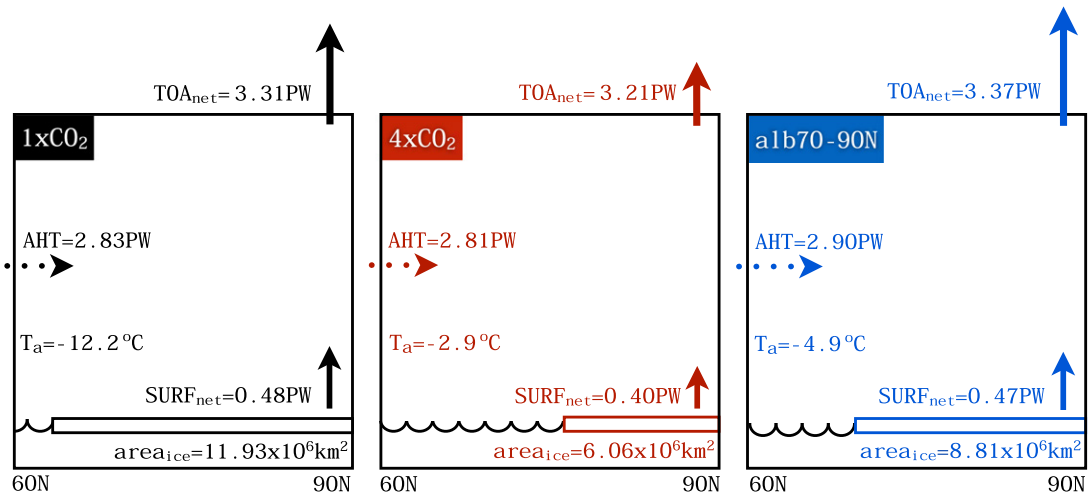


**Figure 4.** Schematic illustrating high latitude (60°–90°N) annual mean energy budgets in 1x$CO_2$ (black), 4x$CO_2$ (red) and alb70–90N (4x$CO_2$ simulation with albedo modifications imposed between 70° and 90°N) (blue). Albedo modifications and sea ice recovery in alb70–90N lead to increased surface energy loss relative to the 4x$CO_2$ simulation, which almost equals the 1x$CO_2$ energy loss. Top-of-atmosphere (TOA) high latitude energy loss and northward atmospheric heat transport (AHT) across 60°N in alb70–90N are greater than in either 1x$CO_2$ or 4x$CO_2$ simulations. Resulting ice areas are indicated in lower right corners.

surface (0.21 ± 0.01 PW). Approximately 36% of this increase in surface net shortwave flux is compensated by a reduction in latent heat flux, ~17% by a decrease in net longwave flux to the atmosphere and ~14% by a reduction in sensible heat fluxes (supplementary figure 8(a) and table 5 available at stacks.iop.org/ERL/10/044020/mmedia). Thus the actual increase in net surface energy loss is only one third (~0.07 PW) of the increase in its shortwave component.

High latitude TOA net energy loss in alb70–90N is higher than that in either the 4x$CO_2$ or 1x$CO_2$ simulations and equals 3.37 ± 0.01 PW (compared to 3.31 ± 0.01 and 3.21 ± 0.01 PW in 1x$CO_2$ and 4x$CO_2$ respectively; supplementary table 4 available at stacks.iop.org/ERL/10/044020/mmedia). In a warm 4x$CO_2$ climate relative to 1x$CO_2$, there is a substantial decrease in high latitude shortwave flux to space (supplementary table 6 available at stacks.iop.org/ERL/10/044020/mmedia). Although this is partially compensated by an increase in longwave flux to space, the net energy emitted from the top of the model decreases. Imposed albedo modifications in alb70–90N mainly affect the shortwave fluxes, leading to a large increase in shortwave flux to space and only a small decrease in longwave flux to space (relative to the 4x$CO_2$ simulation). As a result, net flux to space is larger in alb70–90N than in 1x$CO_2$ or 4x$CO_2$ simulations. TOA flux changes are illustrated in supplementary figure 8b (available at stacks.iop.org/ERL/10/044020/mmedia).

Enhanced TOA energy flux to space of 0.16 ± 0.01 PW in alb70–90N relative to 4x$CO_2$ is balanced by the increase in surface net energy flux to the atmosphere of 0.07 ± 0.01 PW and by increased northward AHT across 60°N of 0.09 ± 0.01 PW (figure 4). Increased AHT into the northern high latitudes is a result of increased dry static energy transport. Sea ice restoration not only results in Arctic cooling but also affects the pole-to-equator temperature gradient, leading to increased dry static energy transport from the lower latitudes (Cvijanovic *et al* 2011, Hwang *et al* 2011, Kay *et al* 2012). Latent heat transport is not substantially affected by the sea ice changes (notable latent heat transport changes are only present when increasing the $CO_2$ concentration). Increased northward AHT from the lower latitudes is present in all simulations with imposed albedo modifications (supplementary table 7 available at stacks.iop.org/ERL/10/044020/mmedia), demonstrating that impacts of a large-scale sea ice restoration would extend far beyond the region of altered albedo. Dry static energy, latent heat and AHT anomalies are shown in supplementary figure 9 available at stacks.iop.org/ERL/10/044020/mmedia. Detailed discussion of the energy flux and transport changes is provided in the supplementary material, sections a, b and d available at stacks.iop.org/ERL/10/044020/mmedia.

## 5. Conclusions

In this study we focus on a physical understanding of the impacts of high latitude ocean albedo alteration on sea ice restoration and climate. In this scenario, ocean albedo increase results in high latitude surface energy budget changes and surface cooling that is then spread aloft and southward. This is physically very different from the approaches aimed at blocking solar radiation (by for example, sulfate aerosol injection into the stratosphere), where cooling is achieved by altering the TOA energy budget. While previous studies (Caldeira and Wood 2008, Tilmes *et al* 2014) have demonstrated that the TOA high latitude energy budget modifications can have a substantial effect on sea ice cover, it is not clear if surface methods are able to effectively restore sea ice or decrease high latitude warming.

Our idealized model simulations suggest that imposing surface albedo changes over a large area in the Arctic could lead to partial sea ice recovery in a warm 4xCO2 climate (figure 1(a)). With the most extreme albedo changes (ocean albedo prescribed to 0.9), imposed over the area 70°–90°N, September sea ice area stabilizes at ~40% of preindustrial 1x$CO_2$ sea ice area. In comparison, in the 4x$CO_2$ simulation with no albedo modifications September sea ice area stabilizes at ~3% of preindustrial value. If the albedo over the area 70°–90°N is instead prescribed to equal 0.8 or 0.7, September sea ice area recovers to about 28% of its preindustrial 1x$CO_2$ extent in both cases (see supplementary table 8 for details available at stacks.iop.org/ERL/10/044020/mmedia). However, even the most extreme ocean albedo modifications applied in our model simulations, have only a modest impact on Arctic surface air temperatures (figure 1(b)) and permafrost (supplementary material, section e available at stacks.iop.org/ERL/10/044020/mmedia), leading to a high latitude surface air temperature decrease of only ~2.5 °C relative to the situation with no albedo changes.

From the viewpoint of atmospheric teleconnections, there is ample reason for caution, as in all the simulations performed the impacts of sea ice restoration are also felt in the midlatitudes. Our results thus support the view that Artic sea ice changes affect midlatitude precipitation patterns over the western United States.

While this study focuses on atmospheric and cryospheric (sea ice) impacts of high latitude surface energy budget alteration, there is a broad range of other environmental and ecologic implications that would require careful consideration if this analysis is to be taken in a geoengineering context. For example, blocking incoming solar energy from entering the ocean could have a large impact on the marine biosphere in the Arctic Ocean, while the long term implementation of any high latitude geoengineering could affect the ice sheet mass balance and stability. While our model results imply that ocean albedo alteration does not appear to be an effective way of offsetting the overall effects of $CO_2$ induced global warming or achieving full sea ice recovery, we do not exclude that it may represent a possible approach for small-scale (e.g. individual bay or estuary) sea ice restoration. Regional model simulations that can resolve local processes could serve as a useful tool in providing these answers. Stronger impacts of ice albedo alteration may also be possible under lower $CO_2$ concentrations (see supplementary material, section f available at stacks.iop.org/ERL/10/044020/mmedia). Finally, we cannot dismiss the possibility of a strong nonlinear climate response to ocean albedo alteration in which small albedo changes result in a different or stronger response than is the case with large albedo changes analyzed in this study. Another interesting question for future work would be to investigate how the system responds to a smoother albedo change rather than step function changes.

## Acknowledgments

Support for this research was provided by the Fund for Innovative Climate and Energy Research (FICER) and by the Carnegie Institution for Science endowment. Part of this work was performed under the auspices of the US Department of Energy by Lawrence Livermore National Laboratory under Contract DE-AC52-07NA27344. We thank James Begg (Lawrence Livermore National Laboratory) for useful discussions and helpful comments and D Michael and D Rouson (Stanford's Center for Computational Earth and Environmental Science, CEES) for computational support. The authors declare having no competing interests or other interests that might be perceived to influence the results and/or discussion reported in this article.

## References

Allison I, Brandt R E and Warren S G 1993 East Antarctic sea ice: albedo, thickness distribution, and snow cover *J. Geophys. Res. Oceans* **98** 12417–29

Budikova D 2009 Role of Arctic sea ice in global atmospheric circulation: a review *Glob. Planet. Change* **68** 149–63

Caldeira K and Wood L 2008 Global and Arctic climate engineering: numerical model studies *Phil. Trans. R. Soc.* **366** 4039–56

Chapman W L and Walsh J E 2007 Simulations of Arctic temperature and pressure by global coupled models *J. Clim.* **20** 609–32

Church J A *et al* 2013 Sea level change *Climate Change 2013: The Physical Science Basis. Contribution of Working Group I to the Fourth Assessment Report of the Intergovernmental Panel on Climate Change* ed T F Stocker *et al* (Cambridge: Cambridge University Press)

Collins W D *et al* 2006 The Community Climate System Model version 3 (CCSM3) *J. Climate* **19** 2122–43

Crutzen P J 2006 Albedo enhancement by stratospheric sulfur injections: a contribution to resolve a policy Dilemma? *Clim. Change* **77** 211–20

Cvijanovic I, Langen P L and Kaas E 2011 Weakened atmospheric energy transport feedback in cold glacial climates *Clim. Past* **7** 1061–73

Danabasoglu G, Bates S C, Briegleb B P, Jayne S R, Jochum M, Large W G, Peacock S and Yeager S G 2011 The CCSM4 ocean component *J. Clim.* **25** 1361–89

Danabasoglu G and Gent P R 2009 Equilibrium climate sensitivity: is it accurate to use a slab ocean model? *J. Clim.* **22** 2494–9

Deser C, Tomas R, Alexander M and Lawrence D 2010 The seasonal atmospheric response to projected Arctic sea ice loss in the late twenty-first century *J. Clim.* **23** 333–51

Donohoe A and Battisti D S 2011 Atmospheric and surface contributions to planetary albedo *J. Clim.* **24** 4402–18

Field L A, Wadhams P, Root T, Chetty S, Kammen D M, Venkatesh S, van der Heide D and Baum E 2012 Ice911: developing an effective response to climate change in Earth's cryosphere using high albedo materials *AGU fall meeting abstract* (http://adsabs.harvard.edu/abs/2012AGUFM.C51E.04F)

Francis J A, Chan W, Leathers D J, Miller J R and Veron D E 2009 Winter Northern Hemisphere weather patterns remember summer Arctic sea-ice extent *Geophys. Res. Lett.* **36** L07503

Gent P R *et al* 2011 The community climate system model version 4 *J. Clim.* **24** 4973–91

Hunke E C and Lipscomb W H 2008 *CICE: The Los Alamos Sea Ice Model User's Manual* version 4 Tech. Rep. No. LA-CC-06-012 Los Alamos National Laboratory

Hwang Y-T, Frierson D M W and Kay J E 2011 Coupling between Arctic feedbacks and changes in poleward energy transport *Geophys. Res. Lett.* **38** L17704

Irvine P J, Ridgwell A and Lunt D J 2011 Climatic effects of surface albedo geoengineering *J. Geophys. Res. Atmospheres* **116** D24112

Kay J E, Holland M M, Bitz C M, Blanchard-Wrigglesworth E, Gettelman A, Conley A and Bailey D 2012 The influence of local feedbacks and Northward heat transport on the equilibrium Arctic climate response to increased greenhouse gas forcing *J. Clim.* **25** 5433–50

Kirtman B *et al* 2013 Near-term climate change: projections and predictability *Climate Change 2013: The Physical Science Basis. Contribution of Working Group I to the Fourth Assessment Report of the Intergovernmental Panel on Climate Change* ed T F Stocker *et al* (Cambridge: Cambridge University Press)

Knorr W, Prentice I C, House J I and Holland E A 2005 Long-term sensitivity of soil carbon turnover to warming *Nature* **433** 298–301

Larsen J N *et al* 2014 Polar regions *Climate Change 2014: Impacts, Adaptation, and Vulnerability Part B: Regional Aspects Contribution of Working Group II to the Fifth Assessment Report of the Intergovernmental Panel of Climate Change* ed V R Barros *et al* (Cambridge: Cambridge University Press) pp 1567–1612

Latham J *et al* 2012 Marine cloud brightening *Phil. Trans. R. Soc. Math. Phys. Eng. Sci.* **370** 4217–62

Lawrence *et al* 2011 Parameterization improvements and functional and structural advances in version 4 of the community land model *J. Adv. Model. Earth Syst.* **3** M03001

Li C, Notz D, Tietsche S and Marotzke J 2013 The transient versus the equilibrium response of sea ice to global warming *J. Clim.* **26** 5624–36

Neale R B, Richter J, Park S, Lauritzen P H, Vavrus S J, Rasch P J and Zhang M 2013 The mean climate of the community atmosphere model (CAM4) in forced SST and fully coupled experiments *J. Clim.* **26** 5150–68

Peings Y and Magnusdottir G 2014 Response of the wintertime Northern Hemisphere atmospheric circulation to current and projected Arctic sea ice decline: a numerical study with CAM5 *J. Clim.* **27** 244–64

Perovich D K, Grenfell T C, Light B and Hobbs P V 2002 Seasonal evolution of the albedo of multiyear Arctic sea ice *J. Geophys. Res. Oceans* **107** 8044

Perovich D K, Roesler C S and Pegau W S 1998 Variability in Arctic sea ice optical properties *J. Geophys. Res. Oceans* **103** 1193–208

Ridgwell A, Singarayer J S, Hetherington A M and Valdes P J 2009 Tackling regional climate change by leaf albedo bio-geoengineering *Curr. Biol.* **19** 146–50

Robock A, Oman L and Stenchikov G L 2008 Regional climate responses to geoengineering with tropical and Arctic $SO_2$ injections *J. Geophys. Res. Atmos.* **113** D16101

Screen J A and Simmonds I 2010 The central role of diminishing sea ice in recent Arctic temperature amplification *Nature* **464** 1334–7

Screen J A, Simmonds I, Deser C and Tomas R 2013 The atmospheric response to three decades of observed Arctic sea ice loss *J. Clim.* **26** 1230–48

Seitz R 2011 Bright water: hydrosols, water conservation and climate change *Clim. Change* **105** 365–81

Sewall J O and Sloan L C 2004 Disappearing Arctic sea ice reduces available water in the American West *Geophys. Res. Lett.* **31** 06209

Sewall J O 2005 Precipitation shifts over Western North America as a result of declining Arctic sea ice cover: the coupled system response *Earth Interact.* **9** 1–23

Shepherd J G 2009 Working group on geoengineering the climate *Geoengineering the Climate: Science, Governance and Uncertainty* (London: Royal Society) p 98 (RS policy document, 10/29)

Singarayer J S, Ridgwell A and Irvine P 2009 Assessing the benefits of crop albedo bio-geoengineering *Environ. Res. Lett.* **4** 045110

Smith R D *et al* 2010 The Parallel Ocean Program (POP) *Reference Manual: Ocean Component of the Community Climate System Model (CCSM) and Community Earth System Model (CESM)* Los Alamos National Laboratory Tech. Rep. LAUR-01853, p 141 (www.cesm.ucar.edu/models/cesm1.0/pop2/doc/sci/POPRefManual.pdf)

Tilmes S, Jahn A, Kay J E, Holland M and Lamarque J-F 2014 Can regional climate engineering save the summer Arctic sea ice? *Geophys. Res. Lett.* **41** 880–5

Vihma T 2014 Effects of Arctic sea ice decline on weather and climate: a review *Surv. Geophys.* **35** 1175–214

Voigt A, Stevens B, Bader J and Mauritsen T 2014 Compensation of Hemispheric albedo asymmetries by shifts of the ITCZ and tropical clouds *J. Clim.* **27** 1029–45

Vuuren D P van *et al* 2011 The representative concentration pathways: an overview *Clim. Change* **109** 5–31

Wang M and Overland J E 2012 A sea ice free summer Arctic within 30 years: an update from CMIP5 models *Geophys. Res. Lett.* **39** L18501